

Coupled dynamics of information diffusion and disease transmission considering vaccination and time-varying forgetting probability

Lai-Jun Zhao(赵来军), Lu-Ping Chen(陈陆平), Ping-Le Yang(杨平乐), Fan-Yuan Meng(孟凡圆), and Chen Dong(董晨)

Citation: Chin. Phys. B, 2025, 34 (**11**): 118701. DOI: 10.1088/1674-1056/ade067
Chttp://cpb.iphy.ac.cn; http://iopscience.iop.org/cpb

What follows is a list of articles you may be interested in

Effects of information and policy regulation on green behavior propagation in multilayer networks: Modeling, analysis, and optimal allocation

Xian-Li Sun(孙先莉), and Ling-Hua Zhang(张玲华)
Chin. Phys. B, 2025, 34 (**6**): 068704. DOI: 10.1088/1674-1056/adbedf

Dynamics of information diffusion and disease transmission in time-varying multiplex networks with asymmetric activity levels

Xiao-Xiao Xie(谢笑笑), Liang-An Huo(霍良安), Ya-Fang Dong(董雅芳), and Ying-Ying Cheng(程英英)
Chin. Phys. B, 2024, 33 (**3**): 038704. DOI: 10.1088/1674-1056/ad1176

Studying the co-evolution of information diffusion, vaccination behavior and disease transmission in multilayer networks with local and global effects

Liang'an Huo(霍良安) and Bingjie Wu(武兵杰)
Chin. Phys. B, 2024, 33 (**3**): 038702. DOI: 10.1088/1674-1056/ad0114

Impact of individual behavior adoption heterogeneity on epidemic transmission in multiplex networks

Liang'an Huo(霍良安) and Yue Yu(于跃)
Chin. Phys. B, 2023, 32 (**10**): 108703. DOI: 10.1088/1674-1056/acea65

Reverse-feeding effect of epidemic by propagators in two-layered networks

Dayu Wu(吴大宇), Yanping Zhao(赵艳萍), Muhua Zheng(郑木华), Jie Zhou(周杰), Zonghua Liu(刘宗华)
Chin. Phys. B, 2016, 25 (**2**): 028701. DOI: 10.1088/1674-1056/25/2/028701

Coupled dynamics of information diffusion and disease transmission considering vaccination and time-varying forgetting probability

Lai-Jun Zhao(赵来军)[1,2], Lu-Ping Chen(陈陆平)[1], Ping-Le Yang(杨平乐)[1,2,†], Fan-Yuan Meng(孟凡圆)[3], and Chen Dong(董晨)[4]

[1] *Business School, University of Shanghai for Science and Technology, Shanghai* 200093, *China*
[2] *School of Intelligent Emergency Management, University of Shanghai for Science and Technology, Shanghai* 200093, *China*
[3] *Alibaba Research Center for Complexity Sciences, Hangzhou Normal University, Hangzhou* 311121, *China*
[4] *School of Economics and Management, Jiangsu University of Science and Technology, Zhenjiang* 212100, *China*

(Received 14 March 2025; revised manuscript received 15 May 2025; accepted manuscript online 4 June 2025)

Vaccination is critical for controlling infectious diseases, but negative vaccination information can lead to vaccine hesitancy. To study how the interplay between information diffusion and disease transmission impacts vaccination and epidemic spread, we propose a novel two-layer multiplex network model that integrates an unaware–acceptant–negative–unaware (UANU) information diffusion model with a susceptible–vaccinated–exposed-infected-susceptible (SVEIS) epidemiological framework. This model includes individual exposure and vaccination statuses, time-varying forgetting probabilities, and information conversion thresholds. Through the microscopic Markov chain approach (MMCA), we derive dynamic transition equations and the epidemic threshold expression, validated by Monte Carlo simulations. Using MMCA equations, we predict vaccination densities and analyze parameter effects on vaccination, disease transmission, and the epidemic threshold. Our findings suggest that promoting positive information, curbing the spread of negative information, enhancing vaccine effectiveness, and promptly identifying asymptomatic carriers can significantly increase vaccination rates, reduce epidemic spread, and raise the epidemic threshold.

Keywords: information diffusion, epidemic spreading, vaccine immunization, time-varying forgetting probability

PACS: 87.23.Kg, 87.23.Ge, 64.60.aq

DOI: 10.1088/1674-1056/ade067 **CSTR:** 32038.14.CPB.ade067

1. Introduction

Throughout human history, infectious diseases have consistently presented significant challenges to human health and socioeconomic stability.[1,2] With the acceleration of globalization and the continuous advancement of urbanization, the speed and scope of infectious disease transmission have shown astonishing growth.[3] In this context, information as an intangible force has increasingly highlighted its role in the prevention and control of infectious diseases.[4] The dissemination of information can greatly influence public perception, attitudes, and behaviors toward infectious diseases, thus significantly affecting their transmission within populations.[5] Positive and accurate information can encourage the public to take proactive protective measures, reducing the risk of disease spreading, whereas negative and misleading information can induce panic and erroneous behaviors, accelerating the spread of the epidemic.[6] Moreover, the spread of epidemics can act as a major driving force for information dissemination.[7] The outbreak of an epidemic is often accompanied by extensive news coverage, social media discussion, and public attention, all of which can accelerate the speed and expand the breadth of information dissemination. Therefore, there exists a close coupling relationship between information dissemination and epidemic spread. In-depth research on the coupled dynamics of information and epidemic spread is crucial to understanding the interaction mechanisms between the two and for formulating effective control strategies. Furthermore, it is crucial to acknowledge that epidemic spreading predominantly occurs within urban settings, where offline colocation interactions among individuals play a pivotal role.[8] These interactions not only facilitate information dissemination and complex behaviors like vaccination adoptions but also exhibit a pronounced community structure with nontrivial community centers, as evidenced by recent studies.[9] Moreover, the population density of a city significantly influences these offline contact networks, which in turn affect disease transmission dynamics.[10] Thus, a comprehensive understanding of epidemic spreading necessitates considering both the digital multiplex networks and the aforementioned urban interaction elements.

Multiplex networks, as powerful tools for studying the coupling of multiple spreading dynamics, can simultaneously describe the connections and interactions of various types of

†Corresponding author. E-mail: plyang@usst.edu.cn
© 2025 Chinese Physical Society and IOP Publishing Ltd. All rights, including for text and data mining, AI training, and similar technologies, are reserved.

networks. Most scholars have conducted research on the relationship between information and disease spread based on multiplex networks. Velásquez-Rojas *et al*. analyzed the interaction between two different processes on multiplex networks, finding that increasing the speed of information dissemination reduces disease prevalence, whereas increasing the speed of information processing increases disease prevalence.[11] Xie *et al*. use power-law distributions to study the impact of asymmetric activity levels on dynamic propagation, finding that individual activity levels in the disease transmission layer have a greater influence on disease spread than in the information diffusion layer.[12] Wang *et al*. designed a performance metric to assess the impact of seeds on multilayer networks under structural disruption, exploring the underlying information behind multilayer networks from the perspective of influence maximization and its robustness.[13] Feng *et al*. established a double-layer network model of information and infectious disease spread on signed multiplex networks, using the microscopic Markov chain approach to analyze the model and derive the expression of the epidemic threshold, discovering that increasing the proportion of friendly interactive communications can inhibit the spread of epidemics and raise the epidemic threshold.[14] Hu *et al*. consider a self-discovery mechanism for asymptomatic individuals, factoring in scenarios like community nucleic acid testing and self-antigen testing, and find that greater network coupling enhances information dissemination.[15]

From the outset, research on the coupled spread of information and disease primarily focused on the dissemination of single information. For instance, Granell *et al*. studied the impact of self-awareness and mass media on epidemic spread using the UAU-SIS model, revealing some non-linear characteristics of these relationships.[16] Zhan *et al*. analyzed the relationship between the spread of H7N9 and dengue fever information and disease transmission, proposing a nonlinear model based on the SIS process, which categorized the population into those aware of the epidemic and those unaware.[17] Kabir *et al*. divided the population into informed and uninformed groups, proposing the SIR-UA double-layer network model to study the impact of awareness on epidemic spread in two-layer networks with different topological structures.[18] However, as the research progressed, the focus shifted to the impact of positive and negative information dissemination on the spread of infectious diseases in social networks. Wang *et al*. explored the effects of positive and negative preventive information on the spread of the epidemic, finding that the dissemination of positive preventive information can curb the epidemic, while negative preventive information has the opposite effect.[19] Subsequently, Wang *et al*. incorporated the influence of mass media into a co-evolution model within a two-layer network framework, discovering that mass media can indirectly affect the size and threshold of epidemic.[20] Li *et al*., based on this, considered local and global information sources as well as individual differences, concluding that local and global information can improve awareness of personal self-protection, thus inhibiting epidemic spread.[21]

Moreover, information dissemination is not limited to pairwise interactions; higher-order interactions (*e.g*., 2-simplices) are increasingly gaining attention. Sun *et al*. studied the coupling effect of resources and disease, using a resource network composed of random simplicial complexes in the upper resource layer to transmit resources.[22] Li *et al*. proposed a competitive spread model similar to SIS epidemics, where two diseases spread simultaneously and compete, focusing on the impact of higher-order interactions on the critical behaviors of system.[23] Liu *et al*. introduced 2-simplicial complexes into the awareness diffusion layer, while the disease layer employed pairwise physical contact, finding that individual heterogeneity in the physical layer can increase the epidemic threshold and reduce the epidemic spread.[24] However, in these studies, individuals who have acquired positive or negative information must first forget the information and revert to an unknown state before transitioning to a state of acquiring positive or negative information again, often neglecting the direct conversion between positive and negative information states. Additionally, in previous models,[25–29] the forgetting rate was often set as a constant, but in reality, the forgetting rate varies over time (Ebbinghaus forgetting curve). Thus, setting it as a time-dependent variable in the model is particularly appropriate.[30,31]

In the selection of disease transmission models, previous studies predominantly chose the SIS or SIR models.[29,32–35] However, some diseases have a latency period, to make models more realistic, some studies have introduced an E state(exposed state).[36–39] For instance, Ma *et al*. suggested that many infectious diseases spread in social networks through asymptomatic carriers who can transmit the disease just like infected individuals. Therefore, they established a new UAU-SEIR model to study the impact of asymptomatic carriers on epidemic spread.[39] Tomovski *et al*. examined a discrete-time variant of the non-Markovian SEIS model on complex networks, arguing that non-Markovian models can more accurately describe the transmission process, particularly for epidemic analysis.[36]

Furthermore, it is well-known that for highly contagious and dangerous infectious diseases, resources are immediately invested to develop vaccines. After vaccination, individuals in the social network can gain short-term immunity against the disease and enter the vaccinated state (V state), but previous models often neglected the presence of immune individuals in

the network.[36–40] The spread of infectious diseases can be divided into three phases: early, middle, and late. In the early phase, given the limited vaccine resources, the effective use of vaccines to protect the population deserves exploration. In the middle phase, vaccines are relatively abundant, but "vaccine hesitancy" often arises. People's vaccination decisions are frequently swayed by those around them, showing that information can impact vaccination behavior. In this paper, we make the following assumptions about the scenario. We assume that for certain highly variable epidemics, a single vaccination cannot confer permanent immunity. In the early stages of disease transmission, some individuals in the social network have already received the newly developed vaccine(we select a small number of individuals to be vaccinated in the first stage by identifying the critical nodes in the network[41,42]), but the side effects of the first vaccine on the human body are still unknown. Over time, individuals who received the initial vaccine will have different physiological responses due to their personal constitution. Some individuals, due to strong immunity, do not experience adverse reactions, while others may exhibit symptoms such as fever, dizziness, headache, fatigue, vomiting, diarrhea, and allergic reactions.[43,44] Those experiencing adverse reactions can spread negative information about the vaccine, leading to the dissemination of negative preventive information within the social network, which can affect the vaccination rate of the second phase population and the transmission of infectious diseases. Therefore, we assume that there are two types of information in social networks: positive information encourages people to take effective measures to prevent the spread of infectious diseases and to have a positive attitude towards vaccination, while negative information is just the opposite.

Based on the above analysis, we considered positive and negative information, time-varying forgetting probabilities, and information conversion thresholds, and introduced the exposed and vaccinated states of the disease to propose an innovative research model, UANU-SVEIS. This model aims to study the impact of positive and negative preventive information on population vaccination and epidemic spread in the context of vaccination. We constructed a double-layer multiplex network model, where the upper network represents the information dissemination layer and the lower network represents the disease transmission layer. Using the microscopic Markov chain (MMCA) method, we studied the model, derived the state transition equations for each node, and obtained the analytical expression of the epidemic threshold. By comparing the results of the MMCA method with thous of Monte Carlo (MC), we found that MMCA can accurately predict the outbreak of epidemics. Extensive numerical simulations further confirmed the impact of positive and negative preventive information on epidemic spread and revealed key factors affecting epidemic transmission. The main contributions of this paper are as follows: (i) Proposing a novel UANU-SVEIS model that incorporates exposed and vaccinated states in the disease transmission layer, providing a comprehensive framework for understanding the interplay between information dissemination and epidemic spread in the context of vaccination. (ii) Innovating dynamic information dissemination mechanisms, including time-varying forgetting probabilities and positive-negative information conversion thresholds, to accurately reflect real-world scenarios and derive precise analytical expressions of the epidemic threshold using the microscopic Markov chain method. (iii) Exploring the impact of the time-varying forgetting rate compared to the constant forgetting rate on the vaccination rate and epidemic threshold of the entire model, and obtaining precise quantitative relationships. (iv) Conducting extensive simulations to validate the accuracy of the model and exploring the effects of various parameters on vaccination rates, epidemic thresholds, and disease spread, offering crucial theoretical insights for effective epidemic prevention and control strategies.

The structure of this paper is as follows: Section 2 provides a detailed description of the UANU-SVEIS model in multiplex networks. Section 3 explores the application of the MMCA for theoretical analysis of the model and the calculation of the epidemic threshold. Section 4 validates the theoretical findings through extensive numerical simulations and examines the impact of various parameters on epidemic spread and epidemic threshold. Finally, Section 5 presents the conclusions of the paper.

2. Model description

Our UANU–SVEIS model uses a two-layer multiplex network to simulate the interaction between disease transmission and the dissemination of positive and negative information. As shown in Fig. 1, the lower layer of the model represents the spread of the epidemic in a physical contact network, while the upper layer describes the spread of information related to infectious diseases through online social networks. The edges in both layers are unweighted and undirected, and the nodes in the two layers correspond one-to-one, meaning that each individual appears in both the online social network and the physical contact network. However, each individual has different connections to the surrounding individuals in the two layers, resulting in different topological structures for the two networks. Research indicates that people's online social range is often larger than their offline social range,[45,46] implying that the average degree of nodes in the upper network is greater. Additionally, the meanings of the parameters in the model are shown in Table 1.

Table 1. Meanings of the parameters in the model.

Parameter	Meaning
$\delta_{A/N}(t)$	Positive/negative time-varying information forgetting rate, t stands for time step
$\tau_{A/N}$	Forgetting index in the positive/negative information forgetting rate
$v_{A/N}$	Initial value in the positive/negative information forgetting rate
v	Basic immunization rate
$\psi_{A/N}$	Immunization factor for nodes in the A/N state
μ	Probability of transitioning from the I state to the S state in the lower layer
θ	Probability of transitioning from the V state to the S state in the lower layer
ξ	Probability of transitioning from the E state to the V state in the lower layer
γ	Probability of transitioning from the I state to the V state in the lower layer
μ	Probability of transitioning from the I state to the S state in the lower layer
β	Probability of transitioning from the S state to the E state in the lower layer
$\gamma_{A/N}$	Infection decay factor for nodes in the A/N state
σ	Probability of transitioning from the E state to the I state in the lower layer
α	Basic conversion ratio of positive to negative information
$\lambda_{A/N}$	Transmission rate of positive/negative information

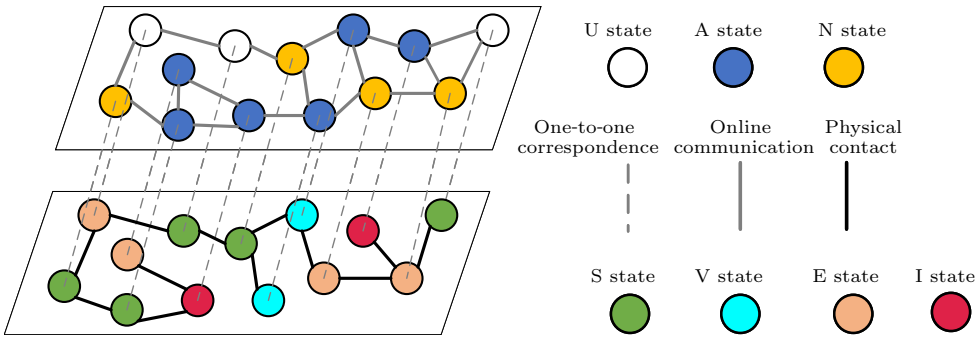


Fig. 1. A schematic diagram of the UANU–SVEIS information-disease coupled model. The upper layer is the information dissemination layer, with three states: Unaware (U), awareness of positive preventive information (A), and awareness of negative preventive information (N). The lower layer is the disease transmission layer, with four states: susceptible (S), exposed (E), infectious (I), and vaccinated (V).

In the upper network, individuals can exist in three possible states: (i) unaware of information related to the infectious disease (U); (ii) aware of positive preventive information and holding a positive attitude towards vaccination (A); and (iii) aware of negative preventive information and holding a negative attitude towards vaccination (N). The transition rules among these states are shown in Fig. 2(a). Individuals in the U state are unaware of any information regarding the spread of the infectious disease and are insensitive to information, so they do not take any preventive measures to avoid infection. Individuals in the A state are aware of the disease information and take positive preventive measures, holding a positive attitude towards vaccination. Compared to individuals in the U state, they are more likely to actively get vaccinated to resist the infectious disease. Individuals in the N state are also aware of the disease information but take negative preventive measures and hold a negative attitude towards vaccination. They are less likely to actively get vaccinated compared to individuals in the U state, and thus have a higher risk of infection. Additionally, individuals in the A or N states will spread their information and viewpoints to their neighbors in the upper information network. Meanwhile, they also have a certain probability of forgetting the information and reverting to the U state. In this paper, the forgetting rate is modeled using the time-varying forgetting rate that we previously employed in our study of rumor propagation.[47] The time-varying function was validated by Gu *et al*. and in line with Ebbinghaus's forgetting curve.[48] This approach aligns with the natural forgetting patterns of individuals, allowing for more realistic research outcomes. The specific expression for the time-varying forgetting rate is

$$\delta(t) = \begin{cases} 0, & v - \mathrm{e}^{-\tau t} < 0, \\ v - \mathrm{e}^{-\tau t}, & 0 \le v - \mathrm{e}^{-\tau t} < 1, \\ 1, & v - \mathrm{e}^{-\tau t} \ge 1, \end{cases} \tag{1}$$

where v is the initial value in the information forgetting rate, τ is the forgetting index in the information forgetting rate, and e is the base of the natural logarithm. The positive and negative time-varying information forgetting rate are denoted by $\delta_A(t)$ and $\delta_N(t)$, respectively. The temporal forgetting probabilities for positive and negative information are captured by adjusting the initial values of v_A, v_N, τ_A, and τ_N.

In the lower network, we use the SVEIS model to characterize the epidemic transmission process. Individuals can exist in one of four possible states: susceptible (S), vaccinated (V), exposed (E), infectious (I). The transition rules for these states are shown in Fig. 2(b). Individuals in the S state are healthy and have not been infected by the disease, but they

may become infected by neighbors who are in the I state or E state. Individuals in the V state have proactively received a vaccine, granting them temporary immunity from the disease, but this immunity does not last indefinitely. Individuals in the E state have been infected but have not yet shown symptoms, while those in the I state have already developed symptoms. Both individuals in I state and E state have the ability to infect their neighbors. The transmission rules for our lower network model are as follows:

(I) Susceptible (S): If individuals in the S state proactively get vaccinated, they transition to the V state, gaining temporary immunity. If they do not get vaccinated, they may be infected by neighbors in the E or I states, transitioning first to the E state upon successful infection.

(II) Exposed (E): Individuals in the E state may transition to the I state after a certain period. However, if they do not transition to the I state and have a strong immune system, they may develop resistance to the disease and transition to the V state through natural active immunity (immunity gained when the body makes its own antibodies after an infection).

(III) Infectious (I): Individuals in the I state will eventually transition back to the S state after a period, and some may also develop natural active immunity, transitioning to the V state.

(IV) Vaccinated (V): After a period, individuals in the V state lose their immunity and transition back to the S state.

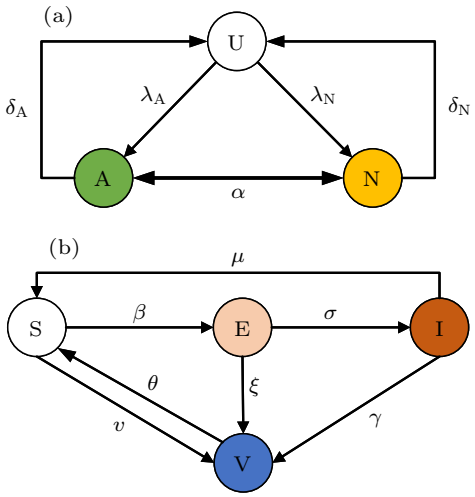


Fig. 2. The meanings of the parameters in this figure can all be found in Table 1: (a) information layer state transition rules and (b) disease layer state transition rules.

Considering the coupling between the information layer and the disease layer, each individual has a total of 12 possible combined states: US, UV, UE, UI, AS, AV, AE, AI, NS, NV, NE, NI. However, when an individual becomes infected (entering the I state) or gains immunity (entering the V state), they immediately recognize the presence of the infectious disease and implement protective measures.[49] Once an individual transitions to the V or I state in the disease layer, their corresponding state in the information layer will be the A state. Therefore, in the proposed model, the combined states of individuals exclude the four states of UV, UI, NV, and NI. We only need to consider eight potential states: US, UE, AS, AE, NS, NE, AI, AV. Each individual transition among these eight states. The models and analyses in this paper are based on four key assumptions:

(i) **Scenario assumption** Individual heterogeneity is not considered. Anyone who actively takes the vaccine can gain temporary immunity to the disease. Also, individuals recovered from infection may acquire temporary immunity with a certain probability. Nevertheless, individuals will eventually return to the susceptible state after a period of time.

(ii) **State assumption** When in the infected (I) or vaccinated (V) state in the disease layer, individuals recognize the disease's presence and adopt proactive defenses, fixing their information layer state to A.

(iii) **Information type assumption** In social networks, individuals have different rates of reception and forgetting for various types of information. People are generally more interested in negative information and tend to remember it more deeply compared to positive information.[50,51] So we set the transmission rate of negative information λ_N higher than that of positive information λ_A. Correspondingly, the forgetting rate of positive information δ_A is higher than that of negative information δ_N.

(iv) **Information influence assumption** The type of information held affects the individual's probability of infection and their likelihood of proactively getting vaccinated. For instance, we set the infection probability for individuals in the U state as β and the proactive vaccination probability as υ. Then, the infection probabilities for individuals in the N and A states are $\beta^N(\beta^N = \gamma_N\beta)$ and $\beta^A(\beta^A = \gamma_A\beta)$ respectively $(0 < \gamma_A < \gamma_N < 1)$. The proactive vaccination probabilities for individuals in the A and N states are $\upsilon^A(\upsilon^A = \psi_A\upsilon)$ $(\psi_A > 1,$ $0 < \psi_A\upsilon < 1)$ and $\upsilon^N(\upsilon^N = \psi_N\upsilon)$ $(0 < \psi_N < 1)$.

3. Theoretical analysis using MMCA

From the basic description of our model in the previous section, we can determine that individuals in our model can be in one of the following eight different states (short as S1, S2, S3, S4, S5, S6, S7, S8):

S1. US (the susceptible state with information unawareness),

S2. UE (the exposed state with information unawareness),

S3. AS (the susceptible state with positive preventive information),

S4. AE (the exposed state with positive preventive information),

S5. NS (the susceptible state with negative preventive information),

S6. NE (the exposed state with negative preventive information),

S7. AI (the infectious state with positive preventive information),

S8. AV (the vaccinated state with positive preventive information).

In this section, we analyze our proposed model from a mathematical perspective. Using the MMCA proposed by Gomez *et al.*,[52] we derive the dynamical equations for epidemic spread under our proposed model. The probability that each node in the network is in a certain state at the next time step can be computed from the probabilities at the current time step. Moreover, since the epidemic threshold of the network is a critical parameter that determines whether an epidemic can spread extensively within the social network and directly reflects the network's ability to resist the spread of infectious diseases, we have calculated the epidemic threshold for our proposed model.

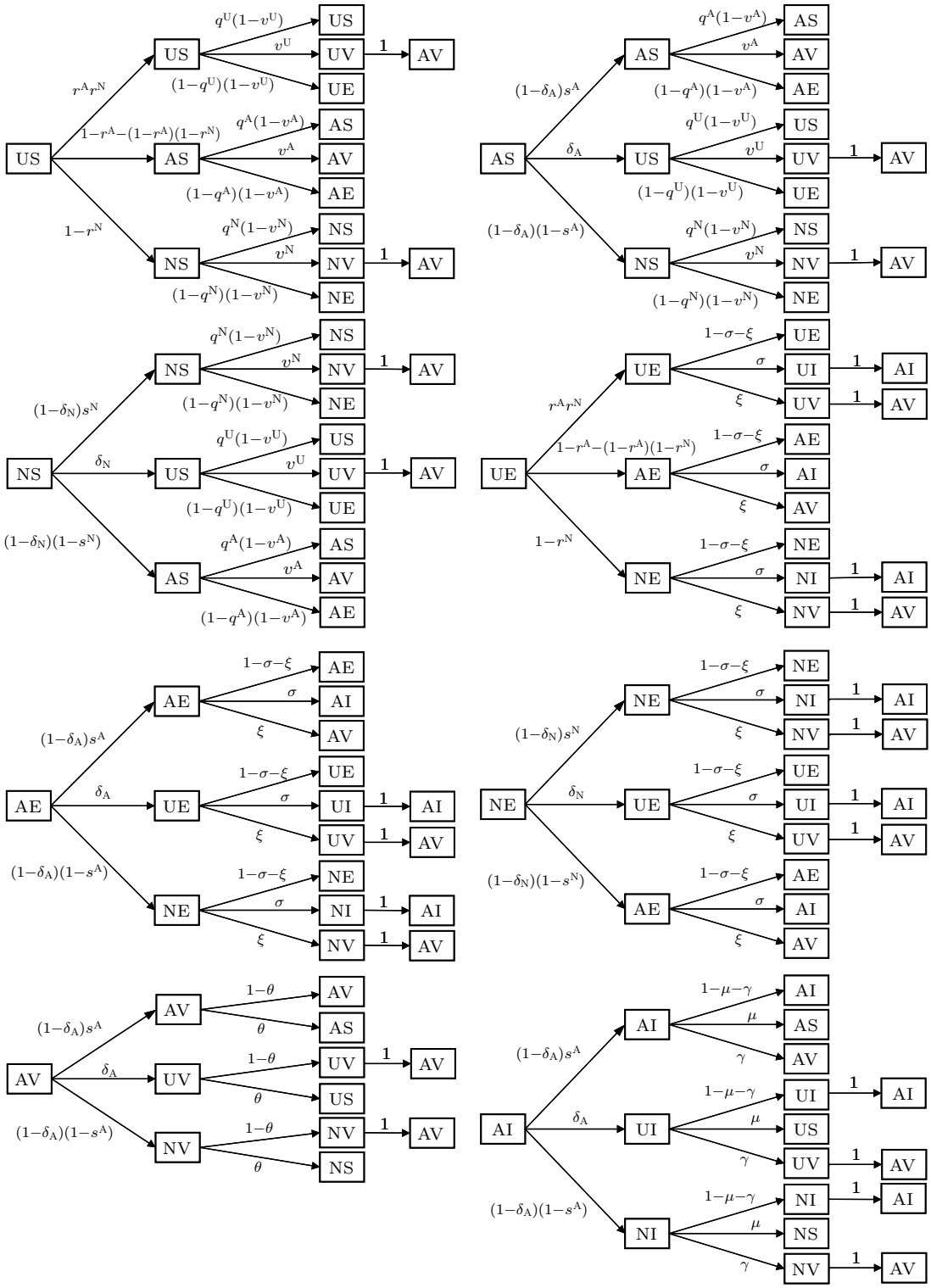


Fig. 3. State transition probability tree containing 8 states US, AS, NS, UE, AE, NE, AI, AV. Each time step is divided into 2 state transition sequences: individual information dissemination and individual disease transmission.

3.1. MMCA equations

Each individual at time t will have a certain probability of being in one of the eight states mentioned above. Therefore, we denote the probabilities that individual i is in each state at time t as follows: $p_i^{\mathrm{US}}(t)$, $p_i^{\mathrm{AS}}(t)$, $p_i^{\mathrm{NS}}(t)$, $p_i^{\mathrm{UE}}(t)$, $p_i^{\mathrm{AE}}(t)$, $p_i^{\mathrm{NE}}(t)$, $p_i^{\mathrm{AI}}(t)$, $p_i^{\mathrm{AV}}(t)$. By summing different terms, we can determine the probability that node i is in a single information or disease state at time t. For example, the probability that node i is in U state at time t is: $p_i^{\mathrm{U}}(t) = p_i^{\mathrm{US}}(t) + p_i^{\mathrm{UE}}(t)$, and the probability that node i is in E state at time t is: $p_i^{\mathrm{E}}(t) = p_i^{\mathrm{UE}}(t) + p_i^{\mathrm{AE}}(t) + p_i^{\mathrm{NE}}(t)$.

We define $A = (a_{ij})$ and $B = (b_{ij})$ as the adjacency matrices of the information dissemination layer and the disease transmission layer, respectively. If nodes i and j have interacted online or offline, then $a_{ij} = 1$; otherwise, $a_{ij} = 0$. If nodes i and j have had physical contact, then $b_{ij} = 1$; otherwise, $b_{ij} = 0$. Furthermore, in the information dissemination layer:

(i) We use $r_i^{\mathrm{A}}(t)$ and $r_i^{\mathrm{N}}(t)$ to denote the probabilities that a node i in U state at time t will not transition to A state and N state, respectively. The formulas are given by Eq. (2) and Eq. (3).

(ii) We use $s_i^{\mathrm{A}}(t)$ to denote the probability that node i in A state at time t will not transition to N state, and $s_i^{\mathrm{N}}(t)$ to denote the probability that node i in N state at time t will not transition to A state. The formulas are given by Eq. (4) and Eq. (5).

In the disease transmission layer, we use $q_i^{\mathrm{U}}(t)$, $q_i^{\mathrm{A}}(t)$, and $q_i^{\mathrm{N}}(t)$ to denote the probabilities that a node i in U state, A state, and N state at time t will not be infected. The formulas are given by Eqs. (6)–(8). The formulas are given as follows:

$$r_i^{\mathrm{A}}(t) = \prod_j (1 - a_{ji} p_j^{\mathrm{A}}(t) \lambda_{\mathrm{A}}), \tag{2}$$

$$r_i^{\mathrm{N}}(t) = \prod_j (1 - a_{ji} p_j^{\mathrm{N}}(t) \lambda_{\mathrm{N}}), \tag{3}$$

$$s_i^{\mathrm{A}}(t) = H\left[\alpha - \frac{\sum_j a_{ji}(p_j^{\mathrm{N}}(t) + p_j^{\mathrm{U}}(t))}{\sum_j a_{ji}}\right], \tag{4}$$

$$s_i^{\mathrm{N}}(t) = H\left[\alpha - \frac{\sum_j a_{ji} p_j^{\mathrm{A}}(t)}{\sum_j a_{ji}}\right], \tag{5}$$

$$q_i^{\mathrm{U}}(t) = \prod_j \left[1 - b_{ji}(p_j^{\mathrm{E}}(t) + p_j^{\mathrm{AI}}(t))\beta_{\mathrm{U}}\right], \tag{6}$$

$$q_i^{\mathrm{A}}(t) = \prod_j \left[1 - b_{ji}(p_j^{\mathrm{E}}(t) + p_j^{\mathrm{AI}}(t))\beta_{\mathrm{A}}\right], \tag{7}$$

$$q_i^{\mathrm{N}}(t) = \prod_j \left[1 - b_{ji}(p_j^{\mathrm{E}}(t) + p_j^{\mathrm{AI}}(t))\beta_{\mathrm{N}}\right]. \tag{8}$$

In the above equations: first, α is a threshold used to control the ease with which individuals transition between positive and negative information states. When α is large, it becomes more difficult for individuals to switch between positive and negative information states. Second, $H(x)$ is a function such that $H(x) = 1$ when $x > 0$, indicating that the individual will continue to maintain their current information state. When $x < 0$, $H(x) = 0$, indicating that the individual will change their current information state.

Since each time step includes two state transition sequences: individual information dissemination and individual disease transmission, we constructed a state transition probability tree to represent the probabilities of each individual transitioning from one of the eight major states to another at the next time step, as shown in Fig. 3. Based on the state transition probability tree, we derive the eight dynamic evolution equations using the MMCA method, as shown below:

$$p_i^{\mathrm{US}}(t+1) = \left[p_i^{\mathrm{US}}(t) r_i^{\mathrm{A}}(t) r_i^{\mathrm{N}}(t) + p_i^{\mathrm{AS}}(t)\delta_{\mathrm{A}}(t) + p_i^{\mathrm{NS}}(t)\delta_{\mathrm{N}}(t)\right] q_i^{\mathrm{U}}(t)(1 - v^{\mathrm{U}}) + \left[p_i^{\mathrm{AV}}(t)\theta + p_i^{\mathrm{AI}}(t)\mu\right]\delta_{\mathrm{A}}(t), \tag{9}$$

$$\begin{aligned} p_i^{\mathrm{AS}}(t+1) = {} & \Big[p_i^{\mathrm{US}}(t)(r_i^{\mathrm{N}}(t) - r_i^{\mathrm{A}}(t) r_i^{\mathrm{N}}(t)) + p_i^{\mathrm{AS}}(t)(1 - \delta_{\mathrm{A}}(t)) s_i^{\mathrm{A}} \\ & + p_i^{\mathrm{NS}}(t)(1 - \delta_{\mathrm{N}}(t))(1 - s_i^{\mathrm{N}})\Big] q_i^{\mathrm{A}}(t)(1 - v^{\mathrm{A}}) + \left[p_i^{\mathrm{AV}}(t)\theta + p_i^{\mathrm{AI}}(t)\mu\right](1 - \delta_{\mathrm{A}}(t)) s_i^{\mathrm{A}}, \end{aligned} \tag{10}$$

$$\begin{aligned} p_i^{\mathrm{NS}}(t+1) = {} & \left[p_i^{\mathrm{US}}(t)(1 - r_i^{\mathrm{N}}(t)) + p_i^{\mathrm{AS}}(t)(1 - \delta_{\mathrm{A}}(t))(1 - s_i^{\mathrm{A}}) + p_i^{\mathrm{NS}}(t)(1 - \delta_{\mathrm{N}}(t)) s_i^{\mathrm{N}}\right] q_i^{\mathrm{N}}(t)(1 - v^{\mathrm{N}}) \\ & + \left[p_i^{\mathrm{AV}}(t)\theta + p_i^{\mathrm{AI}}(t)\mu\right](1 - \delta_{\mathrm{A}}(t))(1 - s_i^{\mathrm{A}}), \end{aligned} \tag{11}$$

$$\begin{aligned} p_i^{\mathrm{UE}}(t+1) = {} & \left[p_i^{\mathrm{US}}(t) r_i^{\mathrm{A}}(t) r_i^{\mathrm{N}}(t) + p_i^{\mathrm{AS}}(t)\delta_{\mathrm{A}}(t) + p_i^{\mathrm{NS}}(t)\delta_{\mathrm{N}}(t)\right](1 - q_i^{\mathrm{U}}(t))(1 - v^{\mathrm{U}}) \\ & + \left[p_i^{\mathrm{UE}}(t) r_i^{\mathrm{A}}(t) r_i^{\mathrm{N}}(t) + p_i^{\mathrm{AE}}(t)\delta_{\mathrm{A}}(t) + p_i^{\mathrm{NE}}(t)\delta_{\mathrm{N}}(t)\right](1 - \sigma - \xi), \end{aligned} \tag{12}$$

$$\begin{aligned} p_i^{\mathrm{AE}}(t+1) = {} & \left[p_i^{\mathrm{US}}(t)(r_i^{\mathrm{N}}(t) - r_i^{\mathrm{A}}(t) r_i^{\mathrm{N}}(t)) + p_i^{\mathrm{AS}}(t)(1 - \delta_{\mathrm{A}}(t)) s_i^{\mathrm{A}} + p_i^{\mathrm{NS}}(t)(1 - \delta_{\mathrm{N}}(t))(1 - s_i^{\mathrm{N}})\right](1 - q_i^{\mathrm{A}}(t))(1 - v^{\mathrm{A}}) \\ & + \left[p_i^{\mathrm{UE}}(t)(r_i^{\mathrm{N}}(t) - r_i^{\mathrm{A}}(t) r_i^{\mathrm{N}}(t)) + p_i^{\mathrm{AE}}(t)(1 - \delta_{\mathrm{A}}(t)) s_i^{\mathrm{A}} + p_i^{\mathrm{NE}}(t)(1 - \delta_{\mathrm{N}}(t))(1 - s_i^{\mathrm{N}})\right](1 - \sigma - \xi), \end{aligned} \tag{13}$$

$$\begin{aligned} p_i^{\mathrm{NE}}(t+1) = {} & \left[p_i^{\mathrm{US}}(t)(1 - r_i^{\mathrm{N}}(t)) + p_i^{\mathrm{AS}}(t)(1 - \delta_{\mathrm{A}}(t))(1 - s_i^{\mathrm{A}}) + p_i^{\mathrm{NS}}(t)(1 - \delta_{\mathrm{N}}(t)) s_i^{\mathrm{N}}\right](1 - q_i^{\mathrm{N}}(t))(1 - v^{\mathrm{N}}) \\ & + \left[p_i^{\mathrm{UE}}(t)(1 - r_i^{\mathrm{N}}(t)) + p_i^{\mathrm{AE}}(t)(1 - \delta_{\mathrm{A}}(t))(1 - s_i^{\mathrm{A}}) + p_i^{\mathrm{NE}}(t)(1 - \delta_{\mathrm{N}}(t)) s_i^{\mathrm{N}}\right](1 - \sigma - \xi), \end{aligned} \tag{14}$$

$$p_i^{\mathrm{AV}}(t+1) = p_i^{\mathrm{US}}(t)\left[r_i^{\mathrm{A}}(t) r_i^{\mathrm{N}}(t) v^{\mathrm{U}} + (r_i^{\mathrm{N}}(t) - r_i^{\mathrm{A}}(t) r_i^{\mathrm{N}}(t)) v^{\mathrm{A}} + (1 - r_i^{\mathrm{N}}(t)) v^{\mathrm{N}}\right]$$

$$+p_i^{\mathrm{AS}}(t)\Big[(1-\delta_{\mathrm{A}}(t))s_i^{\mathrm{A}}v^{\mathrm{A}}+\delta_{\mathrm{A}}(t)v^{\mathrm{U}}+(1-\delta_{\mathrm{A}}(t))(1-s_i^{\mathrm{A}})v^{\mathrm{N}}\Big]$$
$$+p_i^{\mathrm{NS}}(t)\Big[(1-\delta_{\mathrm{N}}(t))s_i^{\mathrm{N}}v^{\mathrm{N}}+\delta_{\mathrm{N}}(t)v^{\mathrm{U}}+(1-\delta_{\mathrm{N}}(t))(1-s_i^{\mathrm{N}})v^{\mathrm{A}}\Big]$$
$$+\Big[p_i^{\mathrm{UE}}(t)+p_i^{\mathrm{AE}}(t)+p_i^{\mathrm{NE}}(t)\Big]\xi+p_i^{\mathrm{AV}}(t)(1-\theta)+p_i^{\mathrm{AI}}(t)\gamma, \tag{15}$$

$$p_i^{\mathrm{AI}}(t+1) = \Big[p_i^{\mathrm{UE}}(t)+p_i^{\mathrm{AE}}(t)+p_i^{\mathrm{NE}}(t)\Big]\sigma+p_i^{\mathrm{AI}}(t)(1-\mu-\gamma). \tag{16}$$

In these equations, $p_i(t)$ represents the probability that an individual is in a particular state at time t, and $p_i(t+1)$ represents the probability that an individual is in a particular state at time $t+1$. The latter can be calculated using arithmetic operations on the former. Additionally, since an individual must be in one of the eight states at any given time, we have the following normalization condition:

$$p_i^{\mathrm{US}}(t)+p_i^{\mathrm{UE}}(t)+p_i^{\mathrm{AS}}(t)+p_i^{\mathrm{AE}}(t)$$
$$+p_i^{\mathrm{NS}}(t)+p_i^{\mathrm{NE}}(t)+p_i^{\mathrm{AI}}(t)+p_i^{\mathrm{AV}}(t)=1.$$

This normalization condition ensures that the sum of the probabilities for all possible states at a given time is equal to 1, reflecting that the individual is always in one of the defined states. This condition is crucial for maintaining the consistency and accuracy of the model's predictions and calculations.

3.2. Epidemic threshold

In this section, we use the eight dynamic evolution equations derived from the Markov chain to calculate the epidemic threshold β_{C}. When the entire system is in a steady state, the probabilities of all nodes being in any of the eight states satisfy the equation $p_i(t+1)=p_i(t)=p_i$. In our model, when a node is infected, its state in the disease layer first transitions to the E state and then from E to I, while its state in the information layer transitions to the A state. Near the epidemic threshold, since the probability of each individual being infected is close to zero, we set $p_i^{\mathrm{E}}=\epsilon_i^{\mathrm{E}}\ll 1$ and $p_i^{\mathrm{I}}=\epsilon_i^{\mathrm{I}}\ll 1$. From Eq. (16), we can derive

$$(\mu+\gamma)p_i^{\mathrm{I}}=\sigma p_i^{\mathrm{E}}, \tag{17}$$

i.e.,

$$\epsilon_i^{\mathrm{I}}=\frac{\sigma}{\mu+\gamma}\epsilon_i^{\mathrm{E}}. \tag{18}$$

Let $\beta^{\mathrm{U}}\sum_j b_{ji}(\epsilon_j^{\mathrm{E}}+\epsilon_j^{\mathrm{I}})=\alpha_i^{\mathrm{U}}$, $\beta^{\mathrm{A}}\sum_j b_{ji}(\epsilon_j^{\mathrm{E}}+\epsilon_j^{\mathrm{I}})=\alpha_i^{\mathrm{A}}$, $\beta^{\mathrm{N}}\sum_j b_{ji}(\epsilon_j^{\mathrm{E}}+\epsilon_j^{\mathrm{I}})=\alpha_i^{\mathrm{N}}$. Then equations (6)–(8) can be approximated as

$$q_i^{\mathrm{U}} = \prod_j\Big(1-b_{ji}(\epsilon_j^{\mathrm{E}}+\epsilon_j^{\mathrm{I}})\beta^{\mathrm{U}}\Big)$$
$$\approx 1-\beta^{\mathrm{U}}\sum_j b_{ji}(\epsilon_j^{\mathrm{E}}+\epsilon_j^{\mathrm{I}})=1-\alpha_i^{\mathrm{U}}, \tag{19}$$

$$q_i^{\mathrm{A}} = \prod_j\Big(1-b_{ji}(\epsilon_j^{\mathrm{E}}+\epsilon_j^{\mathrm{I}})\beta^{\mathrm{A}}\Big)$$
$$\approx 1-\beta^{\mathrm{A}}\sum_j b_{ji}(\epsilon_j^{\mathrm{E}}+\epsilon_j^{\mathrm{I}})=1-\alpha_i^{\mathrm{A}}, \tag{20}$$

$$q_i^{\mathrm{N}} = \prod_j\Big(1-b_{ji}(\epsilon_j^{\mathrm{E}}+\epsilon_j^{\mathrm{I}})\beta^{\mathrm{N}}\Big)$$
$$\approx 1-\beta^{\mathrm{N}}\sum_j b_{ji}(\epsilon_j^{\mathrm{E}}+\epsilon_j^{\mathrm{I}})=1-\alpha_i^{\mathrm{N}}. \tag{21}$$

Next, we derive the expression for the epidemic threshold of the model in three steps:

Step 1 Calculation

Since $p_i^{\mathrm{E}}=p_i^{\mathrm{UE}}+p_i^{\mathrm{AE}}+p_i^{\mathrm{NE}}$, substituting Eqs. (12)–(14) into this, we obtain

$$(\sigma+\xi)p_i^{\mathrm{E}} = [p_i^{\mathrm{US}}r_i^{\mathrm{A}}r_i^{\mathrm{N}}+p_i^{\mathrm{AS}}\delta_{\mathrm{A}}(t)+p_i^{\mathrm{NS}}\delta_{\mathrm{N}}(t)](1-q_i^{\mathrm{U}})(1-v^{\mathrm{U}})+[p_i^{\mathrm{US}}(r_i^{\mathrm{N}}-r_i^{\mathrm{A}}r_i^{\mathrm{N}})$$
$$+p_i^{\mathrm{AS}}(1-\delta_{\mathrm{A}}(t))s_i^{\mathrm{A}}+p_i^{\mathrm{NS}}(1-\delta_{\mathrm{N}}(t))(1-s_i^{\mathrm{N}})](1-q_i^{\mathrm{A}})(1-v^{\mathrm{A}})$$
$$+[p_i^{\mathrm{US}}(1-r_i^{\mathrm{N}})+p_i^{\mathrm{AS}}(1-\delta_{\mathrm{A}}(t))(1-s_i^{\mathrm{A}})+p_i^{\mathrm{NS}}(1-\delta_{\mathrm{N}}(t))s_i^{\mathrm{N}}](1-q_i^{\mathrm{N}})(1-v^{\mathrm{N}}). \tag{22}$$

Step 2 Simplification

Substituting q_i^{U}, q_i^{A}, and q_i^{N} into the expression for p_i^{E}, we obtain

$$(\sigma+\xi)\epsilon_i^{\mathrm{E}} = [p_i^{\mathrm{US}}r_i^{\mathrm{A}}r_i^{\mathrm{N}}+p_i^{\mathrm{AS}}\delta_{\mathrm{A}}(t)+p_i^{\mathrm{NS}}\delta_{\mathrm{N}}(t)]\alpha_i^{\mathrm{U}}(1-v^{\mathrm{U}})+[p_i^{\mathrm{US}}(r_i^{\mathrm{N}}-r_i^{\mathrm{A}}r_i^{\mathrm{N}})$$
$$+p_i^{\mathrm{AS}}(1-\delta_{\mathrm{A}}(t))s_i^{\mathrm{A}}+p_i^{\mathrm{NS}}(1-\delta_{\mathrm{N}}(t))(1-s_i^{\mathrm{N}})]\alpha_i^{\mathrm{A}}(1-v^{\mathrm{A}})$$
$$+[p_i^{\mathrm{US}}(1-r_i^{\mathrm{N}})+p_i^{\mathrm{AS}}(1-\delta_{\mathrm{A}}(t))(1-s_i^{\mathrm{A}})+p_i^{\mathrm{NS}}(1-\delta_{\mathrm{N}}(t))s_i^{\mathrm{N}}]\alpha_i^{\mathrm{N}}(1-v^{\mathrm{N}}). \tag{23}$$

Removing the higher-order terms in ϵ_i for p_i^{US}, p_i^{AS}, p_i^{NS}, and p_i^{AV}, their simplified forms are shown below:

$$p_i^{\mathrm{US}} = \big[p_i^{\mathrm{US}}r_i^{\mathrm{A}}r_i^{\mathrm{N}}+p_i^{\mathrm{AS}}\delta_{\mathrm{A}}(t)+p_i^{\mathrm{NS}}\delta_{\mathrm{N}}(t)\big](1-v^{\mathrm{U}})+p_i^{\mathrm{AV}}\theta\delta_{\mathrm{A}}(t), \tag{24}$$

$$p_i^{\mathrm{AS}} = \left[p_i^{\mathrm{US}}(r_i^{\mathrm{N}} - r_i^{\mathrm{A}} r_i^{\mathrm{N}}) + p_i^{\mathrm{AS}}(1-\delta_{\mathrm{A}}(t))s_i^{\mathrm{A}} + p_i^{\mathrm{NS}}(1-\delta_{\mathrm{N}}(t))(1-s_i^{\mathrm{N}})\right](1-v^{\mathrm{A}}) + p_i^{\mathrm{AV}}\theta(1-\delta_{\mathrm{A}}(t))s_i^{\mathrm{A}}, \tag{25}$$

$$p_i^{\mathrm{NS}} = \left[p_i^{\mathrm{US}}(1-r_i^{\mathrm{N}}) + p_i^{\mathrm{AS}}(1-\delta_{\mathrm{A}}(t))(1-s_i^{\mathrm{A}}) + p_i^{\mathrm{NS}}(1-\delta_{\mathrm{N}}(t))s_i^{\mathrm{N}}\right](1-v^{\mathrm{N}}) + p_i^{\mathrm{AV}}\theta(1-\delta_{\mathrm{A}}(t))(1-s_i^{\mathrm{A}}), \tag{26}$$

$$\begin{aligned} p_i^{\mathrm{AV}}\theta = {} & p_i^{\mathrm{US}}\left[r_i^{\mathrm{A}}(t)r_i^{\mathrm{N}}(t)v^{\mathrm{U}} + (r_i^{\mathrm{N}}(t) - r_i^{\mathrm{A}}(t)r_i^{\mathrm{N}}(t))v^{\mathrm{A}} + (1-r_i^{\mathrm{N}})v^{\mathrm{N}}\right] + p_i^{\mathrm{AS}}\left[(1-\delta_{\mathrm{A}}(t))s_i^{\mathrm{A}}v^{\mathrm{A}} + \delta_{\mathrm{A}}(t)v^{\mathrm{U}} + (1-\delta_{\mathrm{A}}(t))(1-s_i^{\mathrm{A}})v^{\mathrm{N}}\right] \\ & + p_i^{\mathrm{NS}}\left[(1-\delta_{\mathrm{N}}(t))s_i^{\mathrm{N}}v^{\mathrm{N}} + \delta_{\mathrm{N}}(t)v^{\mathrm{U}} + (1-\delta_{\mathrm{N}}(t))(1-s_i^{\mathrm{N}})v^{\mathrm{A}}\right]. \end{aligned} \tag{27}$$

Step 3 Substitution

Expressing p_i^{E} in terms of p_i^{US}, p_i^{AS}, p_i^{NS}, and p_i^{AV}, we obtain

$$\begin{aligned} (\sigma+\xi)\epsilon_i^{\mathrm{E}} = {} & \frac{\alpha_i^{\mathrm{U}}}{(1-v^{\mathrm{U}})}p_i^{\mathrm{US}} + \frac{\alpha_i^{\mathrm{N}}}{(1-v^{\mathrm{N}})}p_i^{\mathrm{NS}} + \frac{\alpha_i^{\mathrm{A}}}{(1-v^{\mathrm{A}})}p_i^{\mathrm{AS}} - \left[\frac{\alpha_i^{\mathrm{U}}}{(1-v^{\mathrm{U}})}\theta\delta_{\mathrm{A}}(t)\right. \\ & \left. + \frac{\alpha_i^{\mathrm{N}}}{(1-v^{\mathrm{N}})}\theta(1-\delta_{\mathrm{A}}(t))(1-s_i^{\mathrm{A}}) + \frac{\alpha_i^{\mathrm{A}}}{(1-v^{\mathrm{A}})}\theta(1-\delta_{\mathrm{A}}(t))s_i^{\mathrm{A}}\right]p_i^{\mathrm{AV}}. \end{aligned} \tag{28}$$

From our previous settings, we know $\alpha_i^{\mathrm{A}} = \gamma_{\mathrm{A}}\alpha_i^{\mathrm{U}}$, $\alpha_i^{\mathrm{N}} = \gamma_{\mathrm{N}}\alpha_i^{\mathrm{U}}$, $\beta^{\mathrm{U}} = \beta$, $\beta^{\mathrm{U}}\sum_j b_{ji}(\epsilon_j^{\mathrm{E}} + \epsilon_j^{\mathrm{I}}) = \alpha_i^{\mathrm{U}}$, $\epsilon_i^{\mathrm{I}} = \frac{\sigma}{\mu+\gamma}\epsilon_i^{\mathrm{E}}$. Substituting α_i^{U}, α_i^{A}, and α_i^{N} into the equation, we obtain

$$\begin{aligned} (\sigma+\xi)\epsilon_i^{\mathrm{E}} = {} & \left(\frac{1}{1-v^{\mathrm{U}}}p_i^{\mathrm{US}} + \frac{\gamma_{\mathrm{N}}}{1-v^{\mathrm{N}}}p_i^{\mathrm{NS}} + \frac{\gamma_{\mathrm{A}}}{1-v^{\mathrm{A}}}p_i^{\mathrm{AS}} - \left[\frac{1}{1-v^{\mathrm{U}}}\theta\delta_{\mathrm{A}}(t) + \frac{\gamma_{\mathrm{N}}}{1-v^{\mathrm{N}}}\theta\right.\right. \\ & \left.\left. \times(1-\delta_{\mathrm{A}}(t))(1-s_i^{\mathrm{A}}) + \frac{\gamma_{\mathrm{A}}}{1-v^{\mathrm{A}}}\theta(1-\delta_{\mathrm{A}}(t))s_i^{\mathrm{A}}\right]p_i^{\mathrm{AV}}\right)\beta\sum_j b_{ji}\frac{\sigma+\mu+\gamma}{\mu+\gamma}\epsilon_j^{\mathrm{E}}. \end{aligned} \tag{29}$$

Setting α_{ji} as the element of the identity matrix where $\alpha_{ji} = 1$ if $i = j$ and $\alpha_{ji} = 0$ otherwise, and further simplifying Eq. (29), we obtain

$$\begin{aligned} & \sum_j\left(\left(\frac{1}{1-v^{\mathrm{U}}}p_i^{\mathrm{US}} + \frac{\gamma_{\mathrm{N}}}{1-v^{\mathrm{N}}}p_i^{\mathrm{NS}} + \frac{\gamma_{\mathrm{A}}}{1-v^{\mathrm{A}}}p_i^{\mathrm{AS}} - \left[\frac{1}{1-v^{\mathrm{U}}}\theta\delta_{\mathrm{A}}(t) + \frac{\gamma_{\mathrm{N}}}{1-v^{\mathrm{N}}}\theta\right.\right.\right. \\ & \left.\left.\left. \times(1-\delta_{\mathrm{A}}(t))(1-s_i^{\mathrm{A}}) + \frac{\gamma_{\mathrm{A}}}{1-v^{\mathrm{A}}}\theta(1-\delta_{\mathrm{A}}(t))s_i^{\mathrm{A}}\right]p_i^{\mathrm{AV}}\right)b_{ji} - \frac{(\sigma+\xi)(\mu+\gamma)}{\beta_{\mathrm{C}}(\sigma+\mu+\gamma)}\alpha_{ji}\right)\epsilon_j^{\mathrm{E}} = 0. \end{aligned} \tag{30}$$

We define matrix H using the elements represented by Eq. (31), then equation (30) can be described in the form of matrix Eq. (32)

$$\begin{aligned} H = {} & \left[\frac{1}{1-v^{\mathrm{U}}}p_i^{\mathrm{US}} + \frac{\gamma_{\mathrm{N}}}{1-v^{\mathrm{N}}}p_i^{\mathrm{NS}} + \frac{\gamma_{\mathrm{A}}}{1-v^{\mathrm{A}}}p_i^{\mathrm{AS}}\right. \\ & - \left(\frac{1}{1-v^{\mathrm{U}}}\theta\delta_{\mathrm{A}}(t) + \frac{\gamma_{\mathrm{N}}}{1-v^{\mathrm{N}}}\theta(1-\delta_{\mathrm{A}}(t))(1-s_i^{\mathrm{A}})\right. \\ & \left.\left. + \frac{\gamma_{\mathrm{A}}}{1-v^{\mathrm{A}}}\theta(1-\delta_{\mathrm{A}}(t))s_i^{\mathrm{A}}\right)p_i^{\mathrm{AV}}\right]b_{ji}, \end{aligned} \tag{31}$$

$$H\epsilon^{\mathrm{E}} = \frac{(\sigma+\xi)(\mu+\gamma)}{\beta_{\mathrm{c}}(\sigma+\mu+\gamma)}\epsilon^{\mathrm{E}}. \tag{32}$$

Here, $\epsilon^{\mathrm{E}} = (\epsilon_1^{\mathrm{E}}, \epsilon_2^{\mathrm{E}}, \epsilon_3^{\mathrm{E}}, \ldots)^{\mathrm{T}}$. Clearly, the eigenvalue of H equals

$$\frac{(\sigma+\xi)(\mu+\gamma)}{\beta_{\mathrm{c}}(\sigma+\mu+\gamma)},$$

so the epidemic threshold of this model is the minimum value satisfying this condition. Therefore, the epidemic threshold in this model can be expressed by

$$\beta_{\mathrm{c}} = \frac{(\sigma+\xi)(\mu+\gamma)}{\Lambda_{\max}(H)(\sigma+\mu+\gamma)}. \tag{33}$$

In Eq. (33), $\Lambda_{\max}(H)$ is the largest eigenvalue of H. It is evident from this equation that the epidemic threshold β_{c} is related to the network topology and various model parameters. It is influenced not only by the parameters of the information layer but also by the parameters of the disease layer, including the proportion of the population initially vaccinated. In the next section, we will conduct extensive numerical simulations to verify the above theoretical analysis results.

4. Numerical simulations

The experimental simulations in this section will be conducted using MATLAB software. The primary experimental content will focus on the following five points: (i) Use MC and MMCA to predict the changes in node state density in the network. Compare the experimental results to validate the accuracy of MMCA derived from our proposed model. (ii) Change certain parameter values in the information layer and disease layer to predict how the density of vaccinated and infected individuals in the network varies with these parameters. (iii) Allow multiple parameter values in the information layer

and disease layer to vary simultaneously over a wide range, generating a heatmap of changes in the density of vaccinated and infected individuals within the network. (iv) Modify certain key parameter values in the information layer and the disease layer to observe changes in the epidemic threshold of the network. (v) Conduct a comparative analysis of the effects of constant forgetting probability and time-varying forgetting probability on the number of vaccinated individuals and the epidemic threshold in social networks.

We define the proportions of individuals in the disease transmission layer in the S state, V state, E state, and I state as ρ^{S}, ρ^{V}, ρ^{E}, and ρ^{I}, respectively. Thus, ρ^{V} refers to the density of the vaccinated population in the network, and ρ^{I} refers to the density of the infected population in the network. We define the proportions of individuals in the information dissemination layer in the states U, A, and N as ρ^{U}, ρ^{A}, and ρ^{N}, respectively. Thus, ρ^{U} refers to the density of the population unaware of the information in the network, ρ^{A} refers to the density of the population holding positive preventive information in the network, and ρ^{N} refers to the density of the population holding negative preventive information in the network.

For MC, $\rho^{\mathrm{S}} = N_{\mathrm{S}}/N$, $\rho^{\mathrm{U}} = N_{\mathrm{U}}/N$, where N_{S} and N_{U} represent the number of individuals in the network in the S state and U state, respectively (similarly for other states), and N represents the total number of individuals in the network. For MMCA, $\rho^{\mathrm{S}} = \frac{1}{N}\sum_{i=1}^{N} p_i^{\mathrm{S}}$, $\rho^{\mathrm{U}} = \frac{1}{N}\sum_{i=1}^{N} p_i^{\mathrm{U}}$, where p_i^{S} and p_i^{U} represent the probabilities of node i being in the S state and U state, respectively (similarly for other states), and N still represents the total number of individuals in the network.

4.1. Experiment settings

The upper and lower network types in this experiment are both BA networks, each with 1000 nodes. The initial average degree of the generated nodes is 6, and the upper network has 400 more edges than the lower network (since an individual's online social circle is generally larger than their offline social circle). The experimental results are averaged over 100 runs. By referring to the experimental data setup in previous studies,[21,22,39] the initial state settings of the network nodes are as follows: in the disease transmission layer, 10% of individuals are in the V state, 2% are in the I state, 2% are in the E state, and 86% are in the S state. In the information dissemination layer, 10% of individuals are in the N state, 12% are in the A state, and 78% are in the U state. Thus, the initial state probabilities for the eight states of the nodes are set as follows: At time t, the probabilities for individual i being in each state are $p_i^{\mathrm{US}}(t) = 0.76$, $p_i^{\mathrm{AS}}(t) = 0$, $p_i^{\mathrm{NS}}(t) = 0.1$, $p_i^{\mathrm{UE}}(t) = 0.02$, $p_i^{\mathrm{AE}}(t) = 0$, $p_i^{\mathrm{NE}}(t) = 0$, $p_i^{\mathrm{AV}}(t) = 0.1$, $p_i^{\mathrm{AI}}(t) = 0.02$. The initial values of the other main parameters in the model are presented in Table 2.

Table 2. Initial values of the main parameters in the model.

Parameter	Initial value	Parameter	Initial value	Parameter	Initial value
γ_{A}	0.5	σ	0.3	λ_{N}	0.6
γ_{N}	0.9	ξ	0.15	α	0.5
v	0.35	θ	0.2	ν_{A}	1
ψ_{A}	1.6	μ	0.2	ν_{N}	1
ψ_{N}	0.4	γ	0.15	τ_{A}	0.6
β	0.4	λ_{A}	0.1	τ_{N}	0.4

4.2. Experiment results

In this section, we conducted experiments based on the five main points proposed above and obtained reasonable experimental results.

4.2.1. MC simulation

We present the changes in population density under different states with respect to the time step t in the MC simulation. Figure 4(a) depicts the function relationship between the population densities of U state, A state, and N state and the time step t. It can be observed that the population density of A state increases continuously over time until it reaches a threshold, after which it fluctuates slightly around 0.8. The population density of N state initially increases and then decreases until it drops to zero. This occurs because once individuals in the disease layer transition to I state or V state, their state in the information layer immediately changes to A. Therefore, the population density of A state shows rapid growth and remains stable in the later stages. Individuals in N state in the information layer are more susceptible to infection, and once infected, their state in the information layer changes to A, resulting in an initial increase followed by a decrease. Figure 4(b) describes the function relationship between the population densities of S state, V state, E state, and I state and the time step t. The population density of V state shows a positive correlation with the time step until it stabilizes, while the population densities of E state and I state exhibit an initial increase followed by a decrease. This is because the number of individuals in A state in the network increases over time, leading to a higher willingness to vaccinate and a lower probability of infection, which in turn causes the population densities of E state and I state to decrease until they reach a threshold. Meanwhile, we can observe that when the system reaches a steady state, the higher the proportion of individuals in the V state within the network, the lower the proportion of individuals in the I or E state. Therefore, the density of individuals in the V state not only reflects the vaccination status of the population within the network but also reveals the extent of infectious disease transmission.

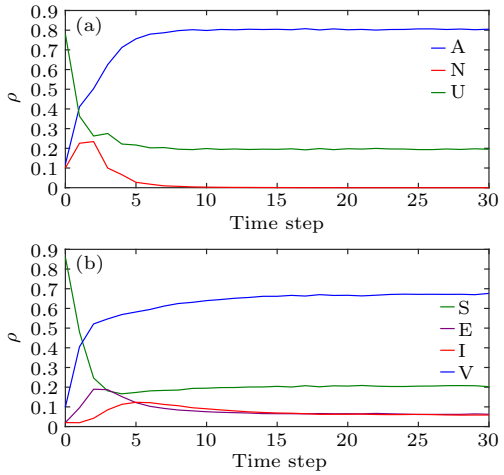


Fig. 4. (a) Population density of U state, A state, and N state over time in MC simulation. (b) Population density of S state, V state, E state, and I state over time in MC simulation.

4.2.2. MC and MMCA mixed simulation

To test the accuracy of the MMCA theoretical analysis in Section 3, we used dynamic equations obtained by MMCA and MC to predict the population density of each state in the network and compared the results. As shown in Fig. 5(a), it depicts the proportional relationship between the population densities of U state, A state, and N state and the infection rate β. Figure 5(b) depicts the proportional relationship between the population densities of S state, V state, E state, and I state and the infection rate β. Clearly, the simulation results of MMCA and MC show a high degree of consistency in both the information and disease layers, with a maximum deviation of 1.9% and a minimum deviation of 0.01% in Fig. 5(a). In Fig. 5(b), the maximum deviation is 2.3% and the minimum deviation is 0.002%. Therefore, the model and analysis results proposed in this paper are highly accurate. In subsequent experimental analyses, we will use the dynamic equations derived from MMCA to predict and analyze the population density in the network.

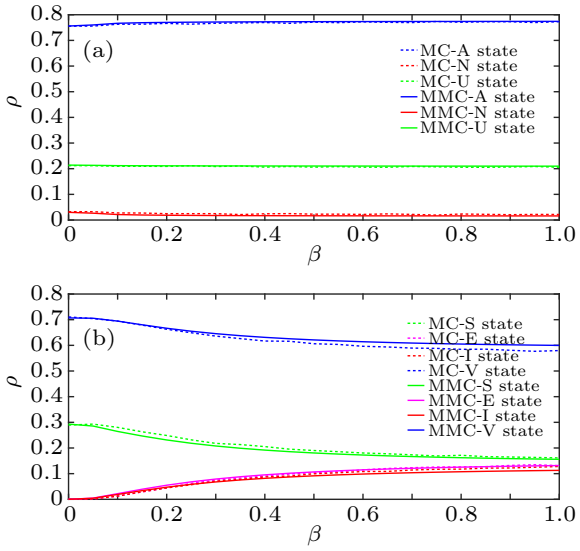


Fig. 5. Comparisons of MC and MMCA mixed simulation results.

4.2.3. Parameter sensitivity analysis

Next, to study the impact of various parameters on epidemic spread, we analyzed the relationship between key parameters in the information and disease layers (σ, μ, λ, and γ) and ρ_V. σ represents the transition rate from E state to I state, μ represents the recovery rate from I state to S state, λ represents the information transmission rate, including both positive and negative information transmission rates, and γ represents the infection decay factor, which differs for positive and negative information. Figure 6 depicts ρ_V as a function of β under different values of σ, μ, λ, and γ. From Figs. 6(a)–6(d), it can be seen that ρ_V decreases as β increases because the higher the probability of infection, the higher the proportion of individuals in I state at equilibrium, resulting in a lower density of V state. Additionally, ρ_V is positively correlated with σ and λ_A and negatively correlated with μ, λ_N, γ_A, and γ_N. Firstly, increasing σ means individuals transition from E state to I state faster, leading to more individuals in I state in the disease layer, which in turn increases the proportion of individuals in A state in the information layer, promoting the spread of positive information about vaccination, and further suppressing the epidemic spread. This effect becomes more pronounced as β increases. Secondly, λ_A is the positive information transmission rate; increasing λ_A also results in more

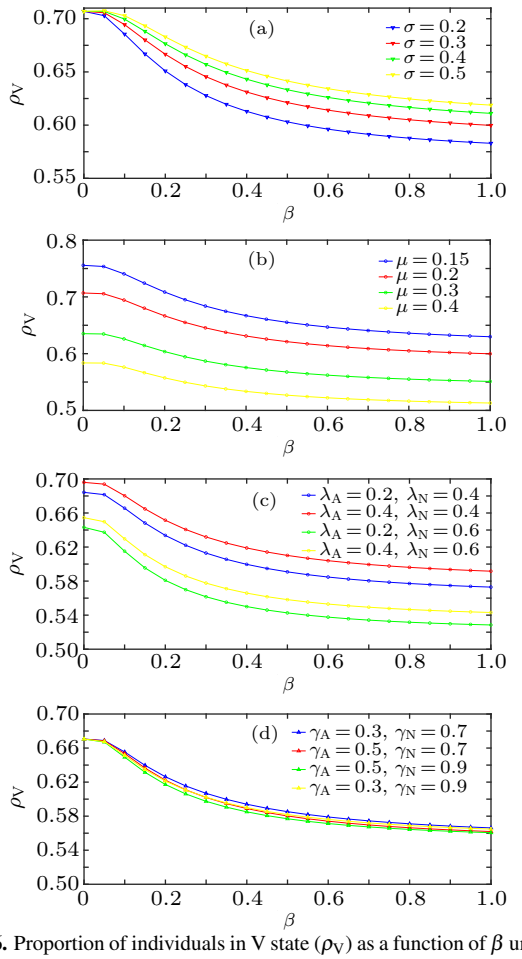


Fig. 6. Proportion of individuals in V state (ρ_V) as a function of β under different values of σ (a), μ (b), λ (c), and γ (d).

individuals getting vaccinated, controlling the number of infections. Thirdly, increasing μ means individuals transition from I state to S state faster, leading to individuals in the information layer potentially transitioning from A state to U state or N state, hindering the spread of positive information, and ultimately reducing ρ_V. On the contrary, it facilitates the spread of infectious diseases. Meanwhile, keeping λ_A constant and increasing λ_N from 0.4 to 0.6 reduces ρ_V by 5%, indicating that the spread of negative information significantly hinders vaccination. Furthermore, whether it is the positive information infection decay factor γ_A or the negative information infection decay factor γ_N, smaller values are more conducive to vaccination because a smaller decay factor means both positive and negative information can greatly encourage people to take preventive measures, reducing the risk of infection, thereby inhibiting the spread of infectious diseases. However, the impact is limited, only causing a slight change in ρ_V.

4.2.4. Mixed parameter sensitivity analysis heatmaps

To further investigate the coupled effects of information transmission parameters and other epidemic parameters on epidemic spread, figures 7–10 show the final vaccination density heatmaps in social networks under different combinations of information layer parameters λ, γ, ψ, and α and important disease layer parameters β, v, and θ. From Figs. 7 and 8, it can be seen that the initial vaccination probability v has a significant impact on the proportion of individuals in V state (ρ_V). When v is set to 0.1, the maximum ρ_V does not exceed 0.5, indicating that less than half of the individuals in the network are vaccinated at equilibrium. When v increases to 0.5, the maximum ρ_V can reach 0.75, and ρ_V continues to increase with v, indicating that increasing the basic willingness of people to vaccinate can most effectively counter the spread of the epidemic.

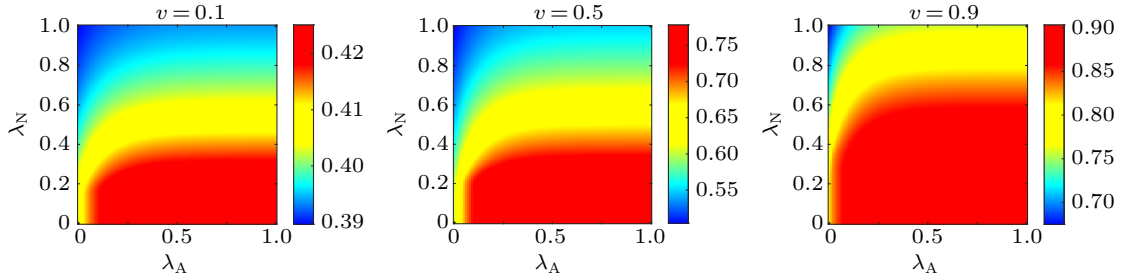


Fig. 7. Full phase diagram of λ_A–λ_N for different values of v. The colors indicate the proportion of individuals in V state (ρ_V) at each point on a 20×20 grid in the steady state.

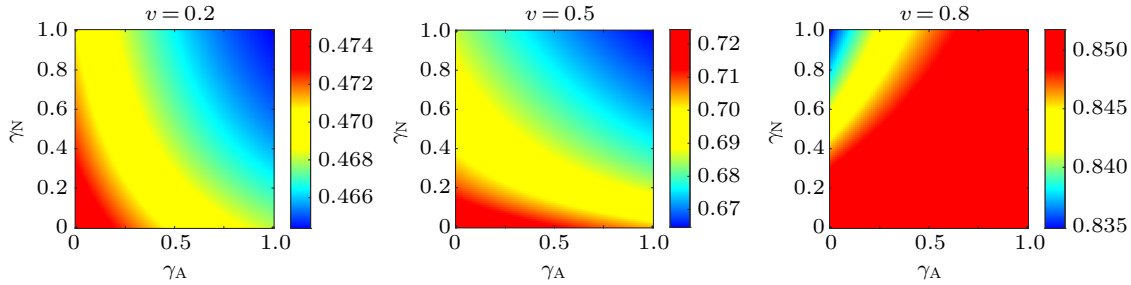


Fig. 8. Different v values full phase diagram γ_A–γ_N. The colors indicate the proportion of individuals in V state (ρ_V) at each point on a 20×20 grid in the steady state.

Figure 7 shows that the inhibitory effect of negative information transmission rate λ_N on ρ_V is more significant than the promoting effect of positive information transmission rate λ_A. This effect is more pronounced at low initial vaccination rates. Therefore, controlling the spread of negative information is crucial. Moreover, as long as positive information can spread in the network when the negative information reception rate is controlled at a low level, a high ρ_V can be achieved. As shown in Fig. 8, the effects of γ_A and γ_N on ρ_V are not significant when v is at a low or high level. This is because when v is low, the probability of individuals getting vaccinated is very low, and regardless of the infection decay factor, individuals will eventually be infected, resulting in ρ_V remaining at a low level with small fluctuations due to changes in the infection decay factor. When v is high, the probability of individuals getting vaccinated is very high, and most individuals get vaccinated before being infected, so the probability of infection does not significantly affect the final ρ_V. When v is at an intermediate level, the effects of changes in γ_A and γ_N on ρ_V are similar.

Figure 9 shows the impact of the initial forgetting rate of information on ρ_V under different initial infection rates. Overall, the change in the initial forgetting rate of information has little effect on ρ_V, and the effect is almost unaffected by β. The maximum fluctuation range of ρ_V does not exceed 0.1. Relatively speaking, changes in the initial forgetting rate

of negative information v_N have little impact on ρ_V. When v_A is less than 1, ρ_V starts to show a slow decline as v_N increases. However, when v_A is greater than 1, this change becomes extremely insignificant. As v_A gradually approaches 1.5 from 0.5, meaning the time-varying forgetting probability of positive information continues to increase, ρ_V gradually decreases and the change becomes noticeable. This indicates that strengthening the promotion of positive information, thereby reducing people's forgetting rate of such information, is crucial for the prevention and control of infectious diseases. Figure 10 studies the coupling effect of immunization factors ψ_A, ψ_N, and vaccination failure rate θ on ρ_V. Overall, the graph shows diagonal symmetry, with a strong correlation between the three and ρ_V. ψ_A, ψ_N, and ρ_V are positively correlated, while θ and ρ_V are negatively correlated. The variation in the value of θ can greatly affect the final value of ρ_V in the network. This is because immunization factors and vaccination failure rate are directly related to the final vaccination rate of the population. Immunization factors control the impact of information on individual willingness to vaccinate, while the immunization failure rate controls the effective time of the vaccine. Therefore, improving the safety, durability, and acceptability of vaccines is crucial for increasing the final vaccination rate in the population and controlling the spread of infectious diseases.

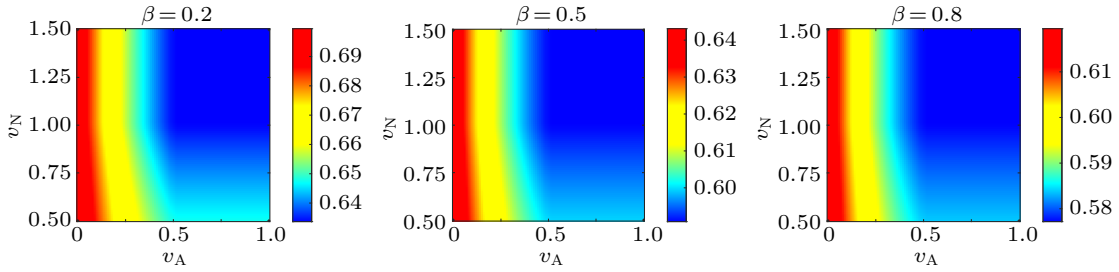


Fig. 9. Different v values full phase diagram v_A–v_N. The colors indicate the proportion of individuals in V state (ρ_V) at each point on a 20×20 grid in the steady state.

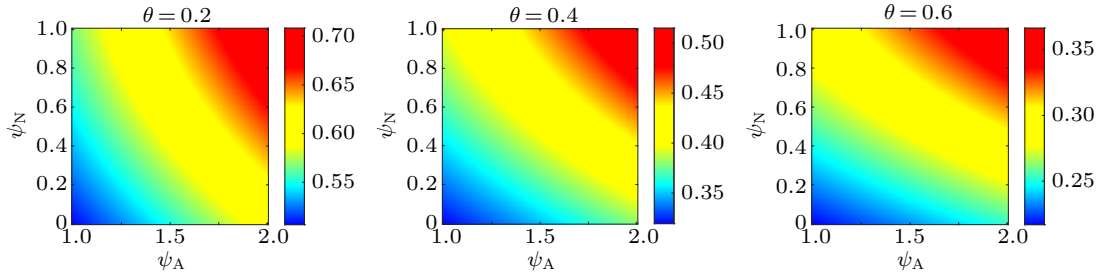


Fig. 10. Different v values full phase diagram ψ_A–ψ_N. The colors indicate the proportion of individuals in V state (ρ_V) at each point on a 20×20 grid in the steady state.

4.2.5. Effect of parameters on epidemic threshold

The epidemic threshold is a key factor in understanding the dynamics of epidemic spread in social networks. In Section 3, we derived the epidemic threshold of the proposed model using MMCA dynamic equations. The expression shows that the epidemic threshold is affected by various parameters. In Fig. 11, we study the coupled effects of information layer parameters λ and ψ and disease layer parameter μ on the epidemic threshold. Firstly, we can see that the epidemic threshold β_c increases with the positive information transmission rate λ_A and decreases with the negative information transmission rate λ_N from Fig. 11(a). Moreover, the higher the λ_A and the lower the λ_N, the greater the increase in β_c. Therefore, strengthening the spread of positive information and curbing the spread of negative information can effectively prevent the outbreak of epidemics. Secondly, as shown in Fig. 11(b), the epidemic threshold β_c increases with the increase in immunization factors (ψ_A and ψ_N). Therefore, enhancing the effectiveness of vaccines against infectious diseases to improve people's willingness to vaccinate is crucial to controlling the spread of epidemics. Furthermore, as shown in Figs. 11(a) and 11(b), the epidemic threshold β_c steadily increases with the recovery rate μ, indicating that improving healthcare, developing effective anti-epidemic drugs, can effectively prevent the outbreak of epidemics.

In Fig. 12, we analyze the coupled effects of γ, v, and σ on the epidemic threshold. Firstly, as shown in Fig. 12(a), the epidemic threshold β_c decreases with the increase in the infection decay factors γ_A and γ_N. This is because when the infection decay factor is large, the impact of information transmission on people's infection is reduced. When the infection decay factor is large, whether individuals acquire positive or negative information about infectious diseases, the probability of infection does not change significantly, making it less ef-

fective in resisting the spread of epidemics in social networks. Secondly, as shown in Fig. 12(b), the epidemic threshold β_c decreases with the increase in the initial information forgetting rate (v_A and v_N). This is because as the speed at which people forget information increases, the number of individuals in U state increases, hindering the spread of information, which is detrimental to suppressing the spread of infectious diseases. In today's information-explosive era, when many other attention-grabbing news events are constantly occurring, people's rate of forgetting information will continue to accelerate. Therefore, when an epidemic begins to spread in a social network, information needs to be controlled to prevent other irrelevant information from diverting attention from the epidemic. Moreover, as σ increases, meaning the transition speed from E state to I state increases, the epidemic threshold β_c steadily increases. This shows that the longer the incubation period of an infectious disease, the harder it is to detect, and the easier it is to spread in the social population.

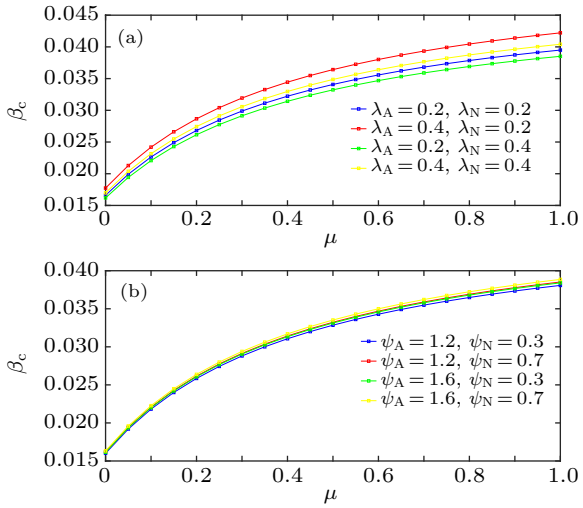


Fig. 11. (a) Epidemic threshold β_c as a function of μ under different values of λ_A and λ_N. (b) Epidemic threshold β_c as a function of μ under different values of ψ_A and ψ_N.

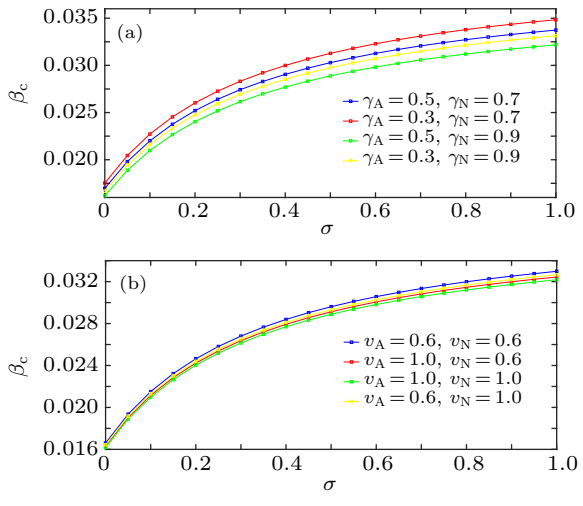


Fig. 12. (a) Epidemic threshold β_c as a function of σ under different values of γ_A and γ_N. (b) Epidemic threshold β_c as a function of σ under different values of v_A and v_N.

4.2.6. Time-varying forgetting probability and constant forgetting probability

Finally, to compare the different changes in the proportion of vaccinated individuals in the population and the epidemic threshold of social networks under the influence of variable forgetting rates and constant forgetting rates in the model selection, we set the parameters in the variable forgetting rate as: $v_A = 1$, $v_N = 1$, $\tau_A = 0.6$, and $\tau_N = 0.4$. The constant forgetting rates are set as the arithmetic mean of these values, i.e., $\delta_A = 0.6$ and $\delta_N = 0.4$. This setup allows for a more meaningful comparison in the experiment.

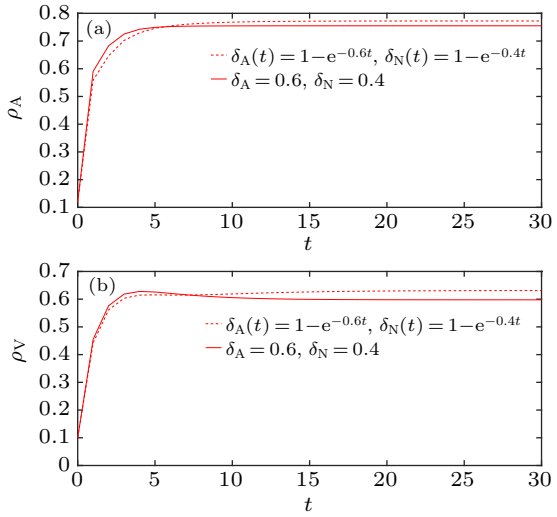


Fig. 13. (a) The time-varying changes in the density of individuals in A state within the information layer of a double-layer coupled network under both variable and constant forgetting rates. (b) The time-dependent changes in the density of individuals in V state within the disease layer of the double-layer coupled network under both variable and constant forgetting rates.

In Fig. 13, we investigate the changes in the density of individuals in A state and V state in the network over time. As shown in Fig. 13(a), when the forgetting rate is constant, the density of individuals in A state grows faster initially and reaches a steady state more quickly. However, the density of individuals in A state after stabilization is lower than that under the variable forgetting rate. This is because in the initial stages, when the forgetting rate is considered a constant, it is higher than people's actual forgetting probability, causing individuals in the N state of the information layer to forget the information and potentially transition to the A state. However, in later stages, the constant forgetting probability becomes lower than the actual forgetting probability of people, which hinders the transition from N state to A state. Similarly, in Fig. 13(b), when the forgetting rate is constant, the density of individuals in V state grows faster initially, then slowly decreases after reaching a peak, and takes longer to reach a steady state. The density of individuals in V state after stabilization is lower than that under the variable forgetting rate. The graph is generally consistent with Fig. 13(a). This is because individuals in V

state in the disease layer are always in A state in the information layer. At the same time, we also studied the changes in the epidemic threshold under the two values of the forgetting rate with respect to the parameters σ and μ. From Figs. 14(a) and 14(b), it is easy to see that when the forgetting rate is constant, it is more conducive to increasing the epidemic threshold of the double-layer coupled network, and as the parameters σ and μ increase, the improvement becomes more significant. Therefore, we can conclude that the variable forgetting rate is more conducive to vaccination, reducing the spread of infectious diseases, while the constant forgetting rate is more conducive to raising the epidemic threshold of the double-layer coupled network, enhancing the network's resistance to infectious diseases.

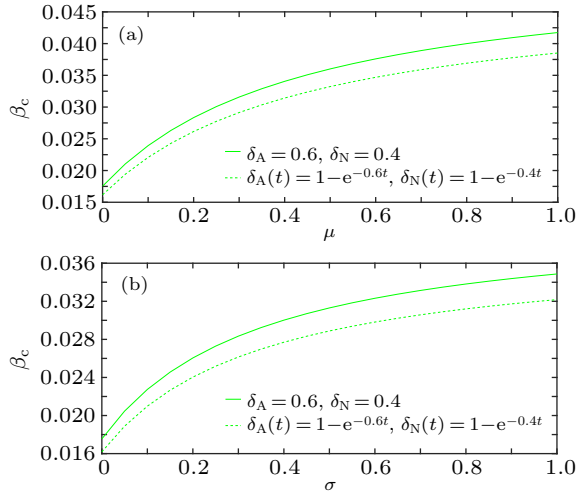


Fig. 14. (a) The epidemic threshold of the double-layer coupled network varies with the parameter μ under both variable and constant forgetting rates. (b) The epidemic threshold of the double-layer coupled network changes with the parameter σ under both variable and constant forgetting rates.

5. Conclusion

In this paper, we construct a UANU–SVEIS information-disease double-layer network model considering the non-permanence of immunization effects and the latency of diseases in the context of mass vaccination. In the information propagation layer, we introduce a time-varying forgetting probability to accurately simulate human memory decay patterns and set an information conversion threshold to allow direct transitions between positive and negative information states held by individuals. In the disease transmission layer, we incorporate the phased vaccine immunization status of individuals and emphasize the latency period of certain diseases. Subsequently, we use the MMCA to establish dynamic transfer equations and derive the epidemic threshold of the model. By comparing the theoretical results from the MMCA method with those from MC simulations, we find a high degree of consistency between the two methods. Furthermore, we investigate the impact of model parameters (positive and negative information reception rates, forgetting probability, infection decay factor, immunization factor, and disease layer-related parameters) on population vaccination, disease transmission, and the epidemic threshold in social network. The results indicate that accelerating the spread of positive information, inhibiting negative information dissemination, and improving vaccine efficacy can significantly increase the vaccination rate within the population, thereby effectively curbing the spread of the epidemic and raising the network epidemic threshold. Moreover, compared to a constant forgetting probability, a time-varying forgetting probability can increase the proportion of vaccinated individuals in the final network, but it is not conducive to raising the epidemic threshold of the network. Our findings contribute to understanding the coupled interactions between information propagation and disease transmission in the context of population vaccine immunization, providing valuable insights and theoretical foundations for epidemic prevention and control in practical applications.

However, this paper also has some limitations. Firstly, to simplify the model, we assume that once individuals are infected or immunized, their information layer state immediately shifts to the positive information state (A state), thus not considering the UV, UI, NV, and NI states. Secondly, we do not account for the dynamic evolution of the network structure. Human social relationships change over time, and both the physical contact layer and the virtual communication layer are dynamic rather than static. In future research, we will consider adding the UV, UI, NV, and NI states and transforming the network into a time-varying dynamic network to make the model more realistic and obtain more accurate results.

Acknowledgements

Project supported by the National Social Science Foundation of China (Grant Nos. 21BGL217 and 22CGL050) and the Philosophy and Social Science Fund of Education Department of Jiangsu Province (Grant No. 2020SJA2346).

References

[1] Sands P, Turabi A E, Saynisch P A and Dzau V J 2016 *Lancet* **388** 2443
[2] Fonkwo P N 2008 *EMBO Rep.* **9** S13
[3] Antrs P, Redding S J and Rossi-Hansberg E 2023 *Am. Econ. Rev.* **113** 939
[4] Li X J, Li C and Li X 2022 *Sci. China Inf. Sci.* **65** 172202
[5] Yang P, Fan R, Wang Y and Zhang Y 2024 *Chin. Phys. B* **33** 070206
[6] Wang W, Nie Y Y, Li W Y, Lin T, Shang M S, Su S, Tang Y, Zhang Y C and Sun G Q 2024 *Phys. Rep.* **1056** 1
[7] Du E H, Chen E, Liu J and Zheng C M 2021 *Sci. Total Environ.* **761** 144114
[8] Liu C X, Yang Y, Chen B S, Cui T Y, Shang F, Fan J F and Li R Q 2022 *Chaos* **32** 081105
[9] Shi D Y, Shang F, Chen B S, Expert P, Lü L Y, Stanley H E, Lambiotte R, Evans T S and Li R Q 2024 *Commun. Phys.* **7** 170
[10] Li R Q, Richmond P and Roehner B M 2018 *Physica A* **510** 713

[11] Velásquez-Rojas F, Ventura P C, Connaughton C, Moreno Y, Rodrigues F A and Vazquez F 2020 *Phys. Rev. E* **102** 022312
[12] Xie X X, Huo L A, Dong Y F and Cheng Y Y 2024 *Chin. Phys. B* **33** 038704
[13] Wang S and Tan X J 2022 *Appl. Soft Comput.* **121** 108750
[14] Feng M L, Liu L J, Chen J X and Xia C Y 2024 *Chaos, Solitons and Fractals* **183** 114858
[15] Hu X, Chen J X and Xia C Y 2024 *Chin. Phys. B* **33** 100202
[16] Granell C, Gómez S and Arenas A 2014 *Phys. Rev. E* **90** 012808
[17] Zhan X X, Liu C, Zhou G, Zhang Z K, Sun G Q, Zhu J J H and Jin Z 2018 *Appl. Math. Comput.* **332** 437
[18] Kabir K M A and Tanimoto J 2019 *Commun. Nonlinear Sci. Numer. Simul.* **72** 565
[19] Wang Z S, Xia C Y, Chen Z Q and Chen G R 2020 *IEEE Trans. Cybern.* **51** 1454
[20] Wang Z S and Xia C Y 2020 *Nonlinear Dyn.* **102** 3039
[21] Li D D, Xie W J, Han D and Sun M 2023 *Inf. Sci.* **651** 119723
[22] Sun Q Y, Wang Z S, Zhao D W, Xia C Y and Perc M 2022 *Chaos, Solitons and Fractals* **164** 112734
[23] Li W Y, Xue X Y, Pan L M, Lin T and Wang W 2022 *Appl. Math. Comput.* **412** 126595
[24] Liu L J, Feng M J, Xia C Y, Zhao D W and Perc M 2023 *Chaos, Solitons and Fractals* **173** 113657
[25] Tian Y and Ding X J 2019 *Appl. Math. Comput.* **363** 124599
[26] Huang S, Chen J, Li M Y, Xu Y H and Hu M B 2024 *Chin. Phys. B* **33** 030205
[27] Huo L A and Wu B J 2024 *Chin. Phys. B* **33** 038702
[28] Chai Y, Wang Y G, Yan J and Sun X L 2023 *Chin. Phys. B* **32** 090202
[29] Yan Z, Zhou X and Du R 2024 *Electron. Commer. Res.* **24** 2021
[30] Murre J M and Dros J 2015 *PloS one* **10** e0120644
[31] Wixted J T 2022 *Proc. Natl. Acad. Sci. USA* **119** e2201332119
[32] Wang S F, Gong M G, Liu W F and Wu Y 2020 *Appl. Soft Comput.* **89** 106118
[33] Zhu Y Y, Shen R Z, Dong H and Wang W 2024 *Chin. Phys. B* **33** 058301
[34] Tan Y P, Cai Y L, Wang X Q, Peng Z H, Wang K, Yao R X and Wang W M 2023 *Math. Comput. Simul.* **204** 1
[35] Sun L H, He Q, Teng Y Y, Zhao Q, Yan X and Wang X W 2023 *Appl. Math. Comput.* **136** 110081
[36] Tomovski I, Basnarkov L and Abazi A 2021 *Physica A* **9** 552
[37] Rădulescu A, Williams C and Cavanagh K 2020 *Sci. Rep.* **10** 21256
[38] Tomovski I, Basnarkov L and Abazi A 2022 *Physica A* **599** 127480
[39] Ma W C, Zhang P, Zhao X and Xue L Y 2022 *Physica A* **588** 126558
[40] Tang L K, Shen R and Pan X Y 2024 *J. Franklin Inst.* **361** 106784
[41] Yang P L, Meng F Y, Zhao L J and Zhou L X 2023 *Chaos, Solitons and Fractals* **166** 112974
[42] Yang P L, Zhao L J, Lu Z, Zhou L X, Meng F Y and Qian Y 2023 *Chaos, Solitons and Fractals* **173** 113720
[43] Zhuang C L, Lin Z J, Bi Z F, Qiu L X, Hu F F, Liu X H, Lin B Z, Su Y Y, Pan H R, Zhang T Y, Huang S J, Hu Y M, Qiao Y L, Zhu F C, Wu T, Zhang J and Xia N S 2021 *Emerg. Microbes Infect.* **10** 365
[44] Rutkowski K, Mirakian R, Till S, Rutkowski R and Wagner A 2021 *Clin. Exp. Allergy* **51** 770
[45] Lieberman A and Schroeder J 2020 *Curr. Opin. Psychol.* **31** 16
[46] Dunbar R I M, Arnaboldi V, Conti M and Passarella A 2015 *Soc. Networks* **43** 39
[47] Zhao L J, Xie W L, Gao H O, Qiu X Y, Wang X L and Zhang S H 2013 *Physica A* **392** 6146
[48] Gu J, Li W and Cai X 2008 *Eur. Phys. J. B* **62** 247
[49] Li L, Dong G G, Zhu H P and Tian L X 2024 *Phys. Rev. Lett.* **472** 128617
[50] Alves H, Koch A and Unkelbach C 2017 *Trends Cogn. Sci.* **21** 69
[51] Ito T A, Larsen J T, Smith N K and Cacioppo J T 1998 *J. Pers. Soc. Psychol.* **75** 887
[52] Gomez S, Arenas A, Borge-Holthoefer J, Meloni S and Moreno Y 2010 *Europhys. Lett.* **89** 38009